

TEAM2024-00025

THE EFFECT OF DEGREASING TEMPERATURE ON THE THICKNESS OF THE FORMED LAYER CREATED BY CATAPHORETIC PAINTING

D. Peti^{1*}, J. Dobransky¹, J. Zajac¹, M. Gombar²

¹Technical University of Kosice, Faculty of Manufacturing Technologies with seat in Presov, Presov, Slovak Republic

²University of West Bohemia Pilsen, Faculty of Mechanical Engineering, Plzen, Czech Republic

*Corresponding author; e-mail: damian.peti@tuke.sk

Abstract

The article investigates the impact of degreasing temperature in the degreasing mixture PRAGOLOD 57N on cataphoretic painting using design of experiments (DoE). Key technological factors such as degreasing deposition time, concentration, cataphoretic deposition time, and voltage are examined for their effect on the thickness of the formed anti-corrosion layer. Cataphoretic painting, an economical and eco-friendly method, is widely used for treating metal parts in automotive and engineering industries. The study involves testing 88 samples, with thickness measurements taken via Elcometer 456C according to the ISO standards and graphical analysis performed using statistical software to optimize the process.

Keywords:

Temperature, degreasing, thickness, layer, cataphoretic painting

1 INTRODUCTION

The researchers Sternadelova et al. [Sternadelova 2023] define electrophoretic paints, also known as cataphoretic painting as organic coatings that disperse in water. These coatings carry an electric charge, allowing the paint to be deposited onto the surface of the metal [Brüggemann 2020]. When the metal sample carries the opposite charge, it results in considerations for formulating its coating [Goldschmidt 2020], [Brock 2010].

Cataphoretic painting, represent cutting-edge technology that results in long-lasting surfaces. These anti-corrosion surfaces not only meet customer expectations in terms of appearance but also enhance efficiency and comply with environmental regulations. These achievements are the culmination of a century of experience, research, and advancements in procedures leading to their theoretical evaluation.

The development of advanced automotive coating and varnish technologies is influenced by factors such as aesthetic properties, anti-corrosion protection, and environmental requirements [Ovsik 2020], [Akafuah 2016]. In the process of cataphoretic painting, cataphoretic colours are released onto surfaces as an electrocoat or paint. These colours are part of organic coatings dispersed in water and carrying an electric charge. This method allows for the application of cataphoretic paint onto specific metal surfaces that have an opposite charge. [Skotnicki 2021], [Jaczewski 2008], [Javidi 2008], [Goeke 2014].

According to the Skotnicki [Skotnicki 2018], the efficacy of an anti-corrosion layer produced through paint coatings like

cataphoretic painting hinges on the interplay of anti-corrosion pigments, the tightness of the coating and its adhesion to the material surface [Maaß 2011]. Surface preparation of the material prior to cataphoretic painting is identified as the pivotal and challenging stage in anti-corrosion technology, involving processes such as degreasing and Zinc-Phosphating [Goeke 2014]. Zinc, known for its cost-effectiveness is a key element utilized in the production of anti-corrosion coatings (Zn, Cu, Ni, Cr) [Grzesik 2016] with the deposition of Zn coatings requiring minimal financial investment [Hashimoto 2016].

The study conducted by Mr. Rossi and colleagues [Rossi 2017] focused on optimizing the application process and assessing the properties of cataphoretic coating on aluminium foam. The impact of the coating on corrosion behavior was evaluated through exposure to an acetic acid salt chamber and electrochemical impedance spectroscopy. By incorporating dye into the resin, three distinct cell types were identified: black cells representing the coating, and light-coloured cells with a purple hue indicating resin residues. The research demonstrated the challenge of achieving uniform coating across the entire aluminium surface in the foam sample. Additionally, a significant discovery was made regarding the deposition voltage, which contributes to the formation of thicker coatings on the formed layer [Votava 2012], [Rossi 2017].

From the second point of view, it is necessary to point out the adverse effects associated with the technological process of cataphoretic painting in accordance with the automotive chain. Authors Kuracal et al. [Kuracal 2019] have investigated that in terms of certain impact categories

that can be characterized as climate change, the main impact arises as a result of the technological process and its use of phase as well as production in the automotive sector. Automotive production processes are divided into four main groups: press, welding, surface coating, and at the end of the automotive chain is assembling. Surface coating, such as cathaphoresis painting operations are among the most important processes as the same as the most polluting part of the manufacturing from both environmental concerns what is related to the high-quality requirements, where the aim is to obtain a clean substrate, free from contaminants such as grease, corrosion products, oils and many others [Chung 2019], [Papasavva 2002]. The supply chain within the technological process of cathaphoresis painting acts as a major contributor to water ecotoxicity, mineral depletion, and toxicity to humans [Rivera 2014], [Hawkins 2013].

Optimizing the cathaphoretic painting process is essential for several key reasons that significantly enhance manufacturing efficiency and product quality. This uniformity is crucial for meeting stringent industrial engineering standards and customer requirements. Moreover, optimalization contributes to environmental sustainability by minimizing waste and energy use. Well-optimized process fosters innovation, strengthens competitive advantage, and enhances customer satisfaction through reliable and timely delivery of high-quality products. The authors of this study recognize the significance of their research in advancing the procedural methodology for the technological application of cathaphoretic painting, leading to the formation of an anti-corrosion layer on the surface. This process involves the manipulation of various parameters, including degreasing temperature which plays a crucial role in ensuring that the surface is adequately prepared for the subsequent coating processes. This leads to a higher quality of the dry layer of KTL and appropriate optimalization of the coating process with enhancing the protective properties of the final product.

2 MATERIAL AND METHODS

2.1 Material selection – VDA239-100 CR4

In order to devise the design of experiments (DOE) for the study at hand, it was imperative to ensure that the material surface remained unaltered, owing to the complexity of specimen preparation.

The German Association of the Automotive Industry (VDA) has promulgated a specification for cold-formed flat steel products. This specification, VDA 239-100, commences with coverage of low-carbon mild steels, such as grades CR3, CR4, and CR5. Owing to their low yield strengths and high ductility, these soft deep-drawing steel grades are particularly well-suited for the fabrication of intricate components. Ductility is quantified by a minimum elongation value; additionally, for CR2, CR3, CR4, and CR5, minimum values are prescribed for the planar anisotropy ratio (r-value) and strain hardening exponent (n-value). Typical applications include demanding exterior and interior automotive body components like fenders, rocker panels, floor pans, spare tire wells, door outers, and inners. The mild steels delineated in VDA 239-100 may be produced as either non-interstitial free (non-IF) or interstitial free (IF) grades. The IF variants exhibit even greater ductility along with exceptionally low carbon and nitrogen contents. Stabilization is achieved through alloying additions of titanium and/or niobium. These deep-drawing steels possess either a fully ferritic microstructure or a ferritic matrix with dispersed granular carbide particles.

Carbonitride, a stabilizer derived from titanium, aids in the removal of ferrite from the interstitial fluids containing carbon and nitrogen atoms. The combination of these components enhances the material's mechanical and plastic qualities.

Tab. 1: Mechanical properties of mild steels acc. VDA 239-100 CR4.

Properties of mild steel CR4	Values
Yield point $R_{p0,2}$ [Mpa]	140 - 180
Tensile strength R_m [Mpa]	270 - 350
Hardness by Brinell HBW	267
Elongation Type 1 A50mm [%]	≥ 40
Elongation Type 2 A80mm [%]	≥ 39
Elongation Type 3 A50mm [%]	≥ 42
r – Value 90/20	$\geq 1,9$
r – Value m/20	$\geq 1,6$
n – Value 10-20/Ag	$\geq 0,20$

Consequently, the selected material of mild steel characterized by the appropriate properties for the designed experiment (DoE) has been a cold-rolled low-carbon steel grade expressly developed for the automotive and general industrial sectors. The steel designation corresponds to VDA239-100 CR4 as per DIN EN 10130 DC05, DC06. The specimen dimensions were predetermined by the Chemcore compendium - 105x190 mm with a sheet thickness of 0,80 mm.

2.2 Measurement methods and devices

The sample preparation for measurement was conducted in accordance with the standard STN EN ISO 1513: 2010.

The Elcometer 456 represents a non-destructive thickness gauge designed for assessing dry coating layers with exceptional precision with an accuracy of $\pm 1\%$ across smooth, rough, thin, and curved surfaces, the device meets stringent international standards, ensuring reliable measurement outcomes. Its enhanced resolution enables precise measurement even for thin coating layers. In the measurement process, a linear ferromagnetic probe denoted as T456CF1S was employed, capable of assessing non-magnetic coatings atop magnetic substrates. This probe's operational range spans from 0 to 1500 μm , ensuring precision within a guaranteed accuracy range of $\pm 1-3\%$ or $\pm 2.5 \mu\text{m}$.

Tab. 2: Characteristics of used probe range T456CF1S.

Range	0 – 60 mils (0-1500 μm)
Accuracy	$\pm 1-3\%$ or $\pm 0,1$ mil ($\pm 2,5 \mu\text{m}$)
Resolution	(0,1 μm : 0-100 μm ; 1 μm : 100-1500 μm)
Min. convex surface radius	4 mm (0,16")
Min. concave surface radius	25 mm (0,98")
Min. headroom	85 mm (3,35")

Using a 3D printing, a specific tool was created into which the cataphoretically treated samples were placed. This tool ensured precise measurement at the same points on each sample. Measurements were conducted in four rows and eight columns, with each point being measured five times. Subsequently, a control measurement was performed using a standard foil with a thickness of 24.1 μm . The total number of measurements for a single sample was 192. The measurements were carried out in accordance with the relevant standard ISO 2808:2019 Paints and varnishes — Determination of film thickness.

2.3 Thickness measurement

The recorded measurement data were processed using Microsoft Excel and the statistical software Statistica. The data were organized into two columns: the first column contained the direct measurements of the thickness of the applied layer, while the second column contained control measurements using a 24.1 μm thick foil standard. Outliers, identified as values that deviated significantly from the majority of measurements in both columns, were excluded using the statistical software, as demonstrated in Fig. 1. Following the removal of these outliers, the average thickness of the applied layer was computed using Statistica and recorded in the corresponding table. The same method was applied to the measurements taken on the foil standard.

Subsequently, the thickness was computed using the control measurements on the standard. This involved subtracting the recorded control measurement from the known foil thickness (24.1 μm), which had been precisely calibrated by the manufacturers. The resultant value was then added to the filtered thickness measurement. This approach facilitated the determination of a relatively accurate average thickness of the applied layer.

Calibration process of the measurement device Elcometer 456 consists of preparation of the probe and gauge, zero calibration, single-point calibration, two-point calibration and verification to verify the accuracy and to provide reliable and accurate measurements, essential for quality control.

Tab. 3 represents an analysis of the model's adequacy and the impact of various factors on the thickness of the deposited cataphoretic layer. The table also reveals that the proportion of variability in the measured thicknesses, as indicated by the R-Squared value, is approximately 75%. The adjusted coefficient of determination (Adjusted R-Squared) in Tab. 3, which assesses the model's effectiveness in capturing the relationship between the input variables (including controlled, chemical, and physical factors) and the observed system response, represented by the layer thickness, suggests that the model explains 70.79% of the variability. From the experimentally measured thicknesses of the cataphoretic layer, it is concluded that the mean thickness (Mean of Response) is 17.71 μm .

Tab. 3: Summary of model fit.

Source	Value
RSquare	0,751148
RSquare Adj	0,707869
Root Mean Square Error	1,922936
Mean of Response	17,71049
Observations (or Sum Wgts)	82

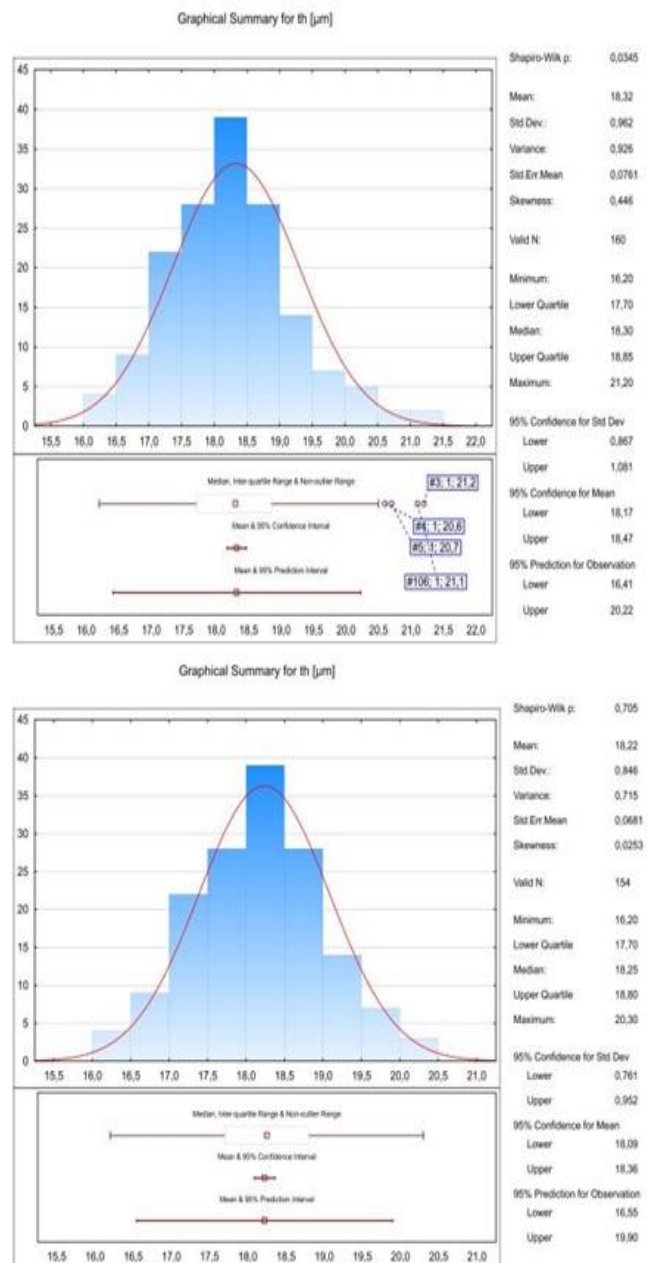


Fig. 1: Filtering gross errors.

Tab. 4: ANOVA – analysis of variance va.

Source	Model	Error	C. Total
DF	12	69	81
Sum of Squares	770,1278	255,1402	1025,268
Mean Square	64,1773	3,6977	-
F Ratio	17,3561	-	-
Prob > F	< 0,0001	-	-

According to Tab. 4, it can be stated that the variability caused by random error is significantly smaller than the variability of measurements explained by the model. The value obtained at the significance level (Prob>F) indicates the adequacy of the model used, as per the Fisher-Snedecor test. The chosen significance level is $\alpha=0.05$. Additionally, it can be asserted that the model is significant.

Tab. 5: Lack of Fit.

Source	Lack of Fit	Pure Error	Total Error
DF	30	39	69
Sum of Squares	135,09267	120,04749	255,14016
Mean Square	4,50309	3,07814	-
F Ratio	1,4629	-	-
Prob > F	0,1312	-	-
Max RSq	0,8829	-	-

The analysis of the Lack of Fit error, as presented in Tab. 5, indicates that the significance level associated with the Lack of Fit test is 0.1312. Therefore, the null statistical hypothesis can be accepted at the chosen significance level of $\alpha=0.05$. This indicates that the variance of the residuals is less than or equal to the variance within groups. Consequently, we can infer that the model is statistically adequate for describing the relationship between the variables under study.

2.4 Parameter of Degreasing temperature – PRAGOLOD 57N

Through systematic analysis and empirical validation, this study seeks to elucidate the role of PragoLOD 57N as a versatile and effective degreasing agent, contributing to advancements in surface treatment methodologies and enhancing the quality and durability of coated products in industrial settings.

PragoLOD 57N is a highly alkaline, low-foaming degreasing agent with medium emulsification properties, primarily designed for immersion and pouring degreasing processes applied to steel and cast-iron surfaces. Its primary function entails the removal of substantial accumulations of preservatives and oily contaminants, as well as persistent adhesives, commonly found on steel substrates. Notably, PragoLOD 57N demonstrates efficacy in dissolving newly developed biodegradable oils derived from acid esters of vegetable oils and rapeseed oils. Additionally, its cleansing action extends to the removal of animal fats and metallic salts of fatty acids. The dispersant present within PragoLOD 57N exhibits effectiveness against both graphic particles and metallic tablecloth residues, which are typically challenging to eliminate from surfaces. Furthermore, its application encompasses degreasing processes involving galvanized articles, as well as light and non-ferrous metal alloys, owing to its uniform adhesion properties.

Tab. 6: Conditions of degreasing mixture PRAGOLOD 57N.

Application	Concentration [%]	Temperature [°C]	Exposure time [min]
Dive	1 - 6	60 - 85	1 - 8
Spray	0,5 - 3	55 - 80	0,5 - 3
Ultrasonund	0,5 - 3	55 - 80	1 - 3

2.5 Technological process of production

The experiment was conducted within the framework of a production process on an automated cathodic electrophoretic deposition line (see Fig. 2). The procedure for preparing each sample prior to the cathodic electrophoretic coating as follows:

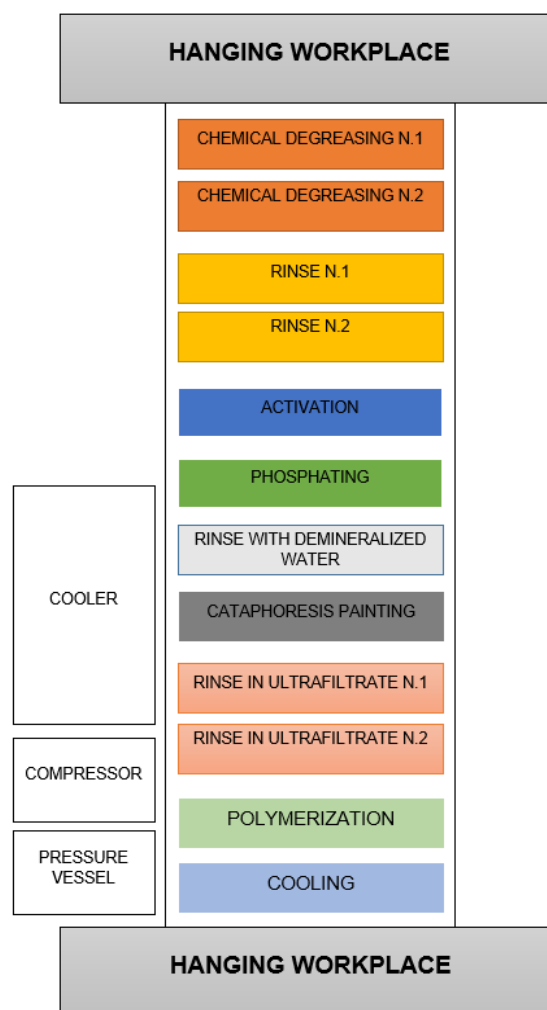


Fig. 2: Automated KTL line for the application of cathodic coatings.

1. Chemical Degreasing Procedure:

Degreasing of samples involves a pivotal step characterized by various parameters such as chemical concentration $[DEGR_{con}]$, temperature and duration of degreasing $[DEGR_{time}] = 3/6/8/10/13$ min. in the process of cathodic painting. This process significantly influences the material's adherence to the substrate. Degreasing is executed in a separate container, away from the cathodic line. The precise amount of chemical is measured using a digital scale and dissolved in water as per experimental requirements. Temperature control is maintained using an electric coil and monitored with a thermometer, while timing is regulated using a stopwatch. Following the designated time interval, samples are extracted from the degreasing solution and subjected to a double rinse in demineralized water.

2. Zinc-Phosphating Procedure:

Phosphating is conducted using a standardized chemical composition, performed inline but away from the operational curtains. Time duration is the chosen variable, with samples immersed for either three or seven minutes in the solution. Phosphate solution temperature, maintained between 50-60 °C, is considered constant. Post-phosphating, samples undergo a two-stage rinse in demineralized water. The resulting phosphate layer forms insoluble crystalline tertiary zinc phosphates on the surface, enhancing anti-corrosion protection and augmenting the adhesion of subsequent cathodic coatings.

3. Cataphoresis Coating Procedure:

Cataphoresis painting is executed utilizing the Cataphoretic line (KTL line). Following phosphating and rinsing, samples are suspended on hangers amidst different coating parts. Painting is performed in a vat, maintaining a constant chemical composition of the paint (solid content). Voltage [KTL_U]= 200/250/300 V and duration are adjusted based on experimental parameters. Real-time monitoring records the temperature, voltage, and current during cataphoresis for comprehensive analysis.

4. Polymerization Procedure:

Polymerization involves altering temperature [DEGR_{temp}]= 40/80 °C, and duration, which are continuously adjustable within the furnace according to experimental specifications. Post-polymerization, samples are allowed to cool, marked, and wrapped in paper. Polymerization directly influences coating hardness.

The primary benefits encompass as limited environmental impact due to the low concentration of solvents (approximately 2%), minimal emission levels, reduced solid waste and wastewater output, exceptional corrosion resistance of the coating, consistent coating thickness across the entire surface, including challenging-to-access areas, edges, and corners, facilitated by the capability for thickness modulation [Holoubek 2005].

3 RESULTS AND DISCUSSION

These findings provide insights into the relationship between various parameters and their impact on the thickness of the deposited layer as observed in Fig. 3.

Effect of Deposition Temperature and Time on Layer Thickness:

- At a maximum degreasing time of 13 minutes and a temperature of approximately 43 °C, the minimum thickness of the layer is observed.
- Maximum layer thickness, approximately 18.10 μm, is observed at a deposition temperature of 80 °C and a degreasing time of 3 minutes.
- Increasing the temperature leads to an increase in layer thickness, reaching 21.03 μm at 80 °C for a deposition time of 13 minutes. Conversely, thickness decreases to 14.98 μm at the same temperature for a deposition time of 3 minutes.
- Deposition time of 8 minutes exhibits minimal influence on layer thickness, ranging from 18.14 μm to 18.01 μm across temperature variations.

Effect of Cataphoretic Deposition Time and Temperature on Layer Thickness:

- Modulating the cataphoretic deposition time reveals that at an initial temperature of 40 °C, a polynomial layer with thickness ranging from 20.05 μm to 20.11 μm is formed.
- Increasing the degreasing time to 13 minutes only marginally increases the thickness by 0.25 μm across the temperature range.
- For a deposition time of 3 minutes, the layer thickness diminishes, reaching 17.52 μm at 80 °C. This indicates that within the degreasing time range of 3 to 10 minutes, higher degreasing temperatures correlate with decreased layer thickness.

Interaction between Deposition Time and Temperature:

- For a deposition time of 7 minutes, the layer thickness diminishes with increasing degreasing temperature across the entire range.

- At 60 °C, a critical point is observed where the maximum thickness occurs at a deposition time of 3 minutes and the minimum at 13 minutes.
- The thickness difference at 40 °C is 0.46 μm, increasing to 0.49 μm at 80 °C.

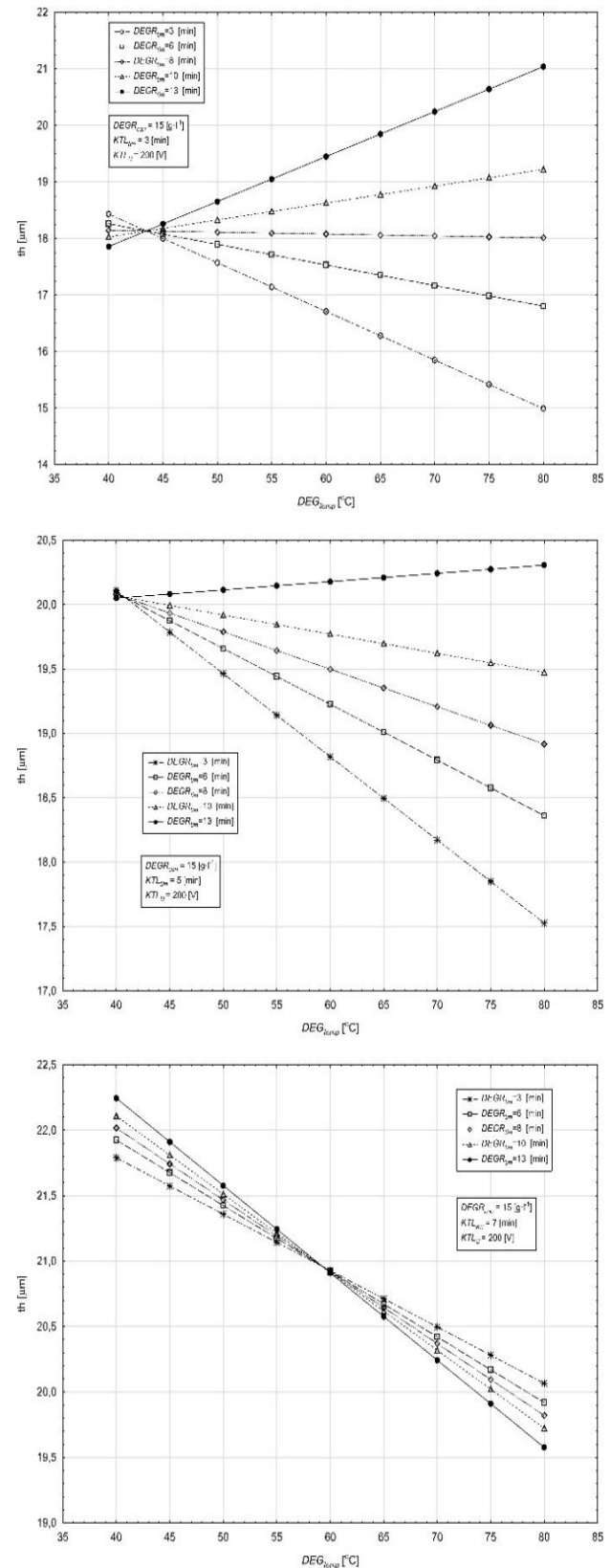


Fig. 3: The influence of the temperature of the degreasing agent and the time of deposition of the degreasing on the change of the created layers at the minimum values of the designed experiment (DoE).

Fig. 4 illustrates the peak values observed in the DoE, delineating the influence of temperature variations contingent upon cataphoretic deposition and degreasing time.

Effect of Cataphoretic Deposition Time and Temperature on Layer Thickness:

- At a cataphoretic deposition time of 3 minutes, increasing temperature correlates with diminishing layer thickness. A critical point is observed at 60 °C, where thickness measures 16.54 μm.
- Maximal thickness is attained with a degreasing time of 3 minutes at 80 °C, yielding a thickness of 15.67 μm. Conversely, the minimum thickness achieved at 80 °C is 15.22 μm.
- At a degreasing temperature of 40 °C and a deposition time of 3 minutes, maximum thickness of 17.88 μm is observed, while the minimum thickness of 17.39 μm is recorded under the same conditions.

Trends Across Different Cataphoretic Deposition Times:

- For a cataphoretic deposition time of 5 minutes, maximum thickness aligns with a degreasing time of 3 minutes at 40 °C, yielding 18.90 μm, while the lowest thickness of 16.12 μm is noted with a degreasing time of 13 minutes.
- Across deposition times of 3, 6, 8, and 10 minutes, increasing degreasing temperature inversely correlates with layer thickness. However, for a deposition time of 13 minutes, higher temperatures correspond to increased thickness.
- At approximately 80 °C, the thickness of the cataphoretic painting layer stabilizes at around 16.35 μm, regardless of degreasing time.

Similar Trends at Different Deposition Times:

- A cataphoretic deposition time of 7 minutes exhibits a similar trend to that of 5 minutes.
- At 40 °C, the maximum thickness of 20.41 μm is achieved with a degreasing time of 3 minutes, while the minimum thickness of 14.36 μm is observed with a deposition time of 13 minutes.
- An inflection point, approximately 76.5 °C, marks a thickness of approximately 17.26 μm, beyond which maximum thickness is reached with a degreasing time of 13 minutes at 80 °C, yielding 17.54 μm.
- Utilizing a degreasing time of 8 minutes yields a consistent layer thickness across temperature variations, with a difference of 0.13 μm.

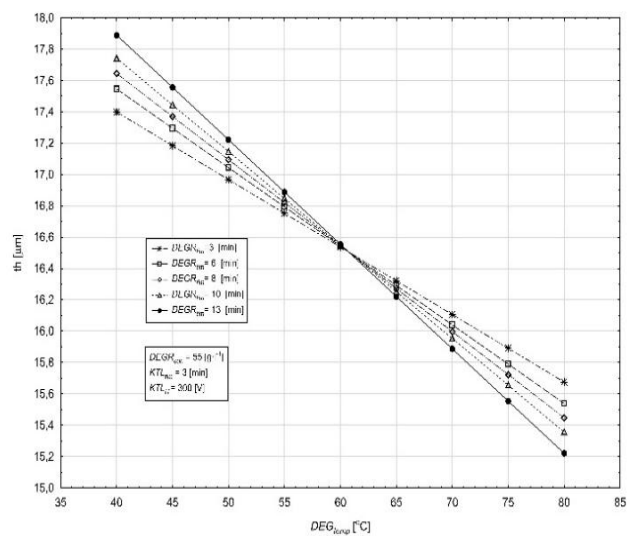
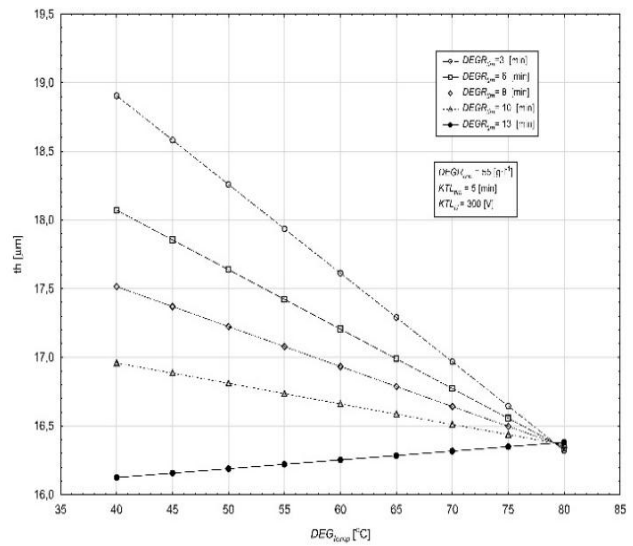
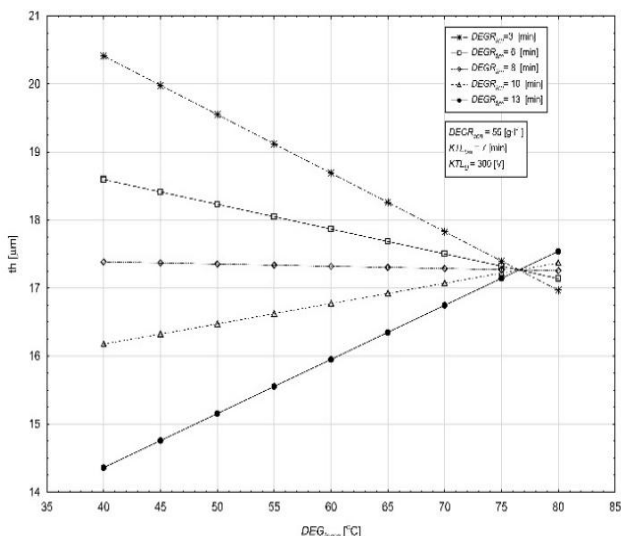


Fig. 4: The influence of the temperature of the degreasing solution and the time of deposition of the degreasing on the change of the created layers at the maximum values of the designed experiment (DoE).

Increasing the temperature of the degreasing solution across the entire temperature spectrum leads to a reduction in the thickness of the formed layer shown in Fig. 5.

Effect of Degreasing Solution Temperature and Concentration on Layer Thickness:

- Increasing the temperature of the degreasing solution leads to a reduction in the thickness of the cataphoretic painting layer across the entire temperature spectrum.
- The maximum thickness of 18.43 μm is achieved at a degreasing temperature of 40°C at a 15 g.L⁻¹.
- This peak shifts as the degreasing temperature reaches 70 °C, resulting in a thickness of 15.85 μm.
- The maximum thickness, reaching 15.44 μm, occurs at a concentration of 55 g.L⁻¹ and 80 °C.
- Conversely, the minimum thickness of 14.82 μm is recorded at 40 °C with a concentration of 35 g.L⁻¹
- The concentration of 35 g.L⁻¹ exhibits the smallest thickness across the temperature range, with a thickness of 12.23 μm at 80 °C.
- The least thickness variation, 1.75 μm, is observed at a concentration of 55 g.L⁻¹, while a concentration of 15 g.L⁻¹ exhibits a thickness variation of 3.45 μm, nearly double of 55 g.L⁻¹.

Effect of Cataphoretic Voltage on Layer Thickness:

- Increasing the cataphoretic voltage to 250 V induces a decreasing trend in thickness across the entire range.
- The highest thickness, 19.92 μm , is achieved at a concentration of 15 g.L^{-1} and a temperature of 40 $^{\circ}\text{C}$, accompanied by the largest thickness range of 3.44 μm between maximum and minimum values.
- Conversely, the lowest thickness of 19.92 μm at 40 $^{\circ}\text{C}$ is observed at a concentration of 35 g.L^{-1} .
- At a concentration of 55 g.L^{-1} and 40 $^{\circ}\text{C}$, a thickness of 17.28 μm is recorded, while at 80 $^{\circ}\text{C}$, a concentration of 55 g.L^{-1} exhibits the lowest thickness variation, reaching 15.55 μm .
- With a maximum cataphoretic voltage of 300 V, the maximum thickness of 21.42 μm is achieved at a concentration of 15 g.L^{-1} and 40 $^{\circ}\text{C}$.
- At 80 $^{\circ}\text{C}$, a concentration of 15 g.L^{-1} yields a layer thickness of 17.97 μm , the greatest thickness loss.
- The second-highest thickness of 18.27 μm at 40 $^{\circ}\text{C}$ results from a concentration of 25 g.L^{-1} .

Crossover and Intersection Points:

- At approximately 67.5 $^{\circ}\text{C}$, a crossover occurs, with a concentration of 55 g.L^{-1} forming the second-highest layer thickness, reaching 15.67 μm at 80 $^{\circ}\text{C}$.
- At 55 $^{\circ}\text{C}$, concentrations of 35 g.L^{-1} and 45 g.L^{-1} intersect, resulting in the lowest layer thickness of 13.85 μm at 80 $^{\circ}\text{C}$.

Overall, the scientific presented analysis provides valuable insights into the factors influencing the cataphoretic painting process, laying the groundwork for further research and process of optimization in automotive and engineering applications of the given technological procedure.

Tab. 7: Technological parameters of the designed experiment (DOE).

Degreasing concentration	[g.L^{-1}]
DEGR _{con}	15//25/35/45/55
Degreasing deposition	[min]
DEGR _{time}	3/6/8/10/13
Cataphoretic deposition	[min]
KTL _{time}	3/5/7
Cataphoretic voltage	[V]
KTL _V	200/250/300

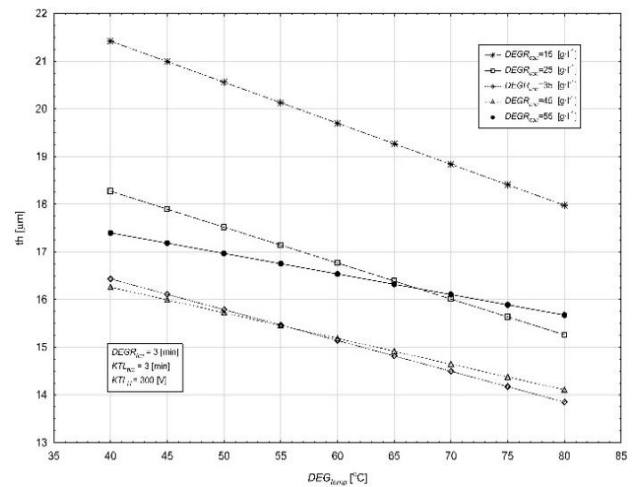
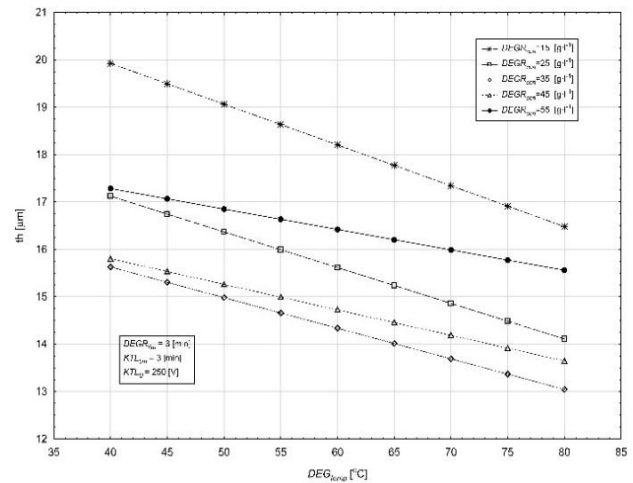
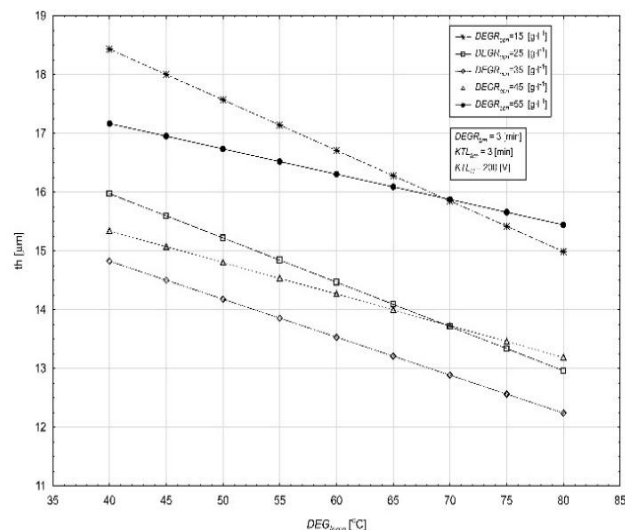


Fig. 5: The influence of the temperature of the degreasing solution and the concentration of the degreasing on the change created layers at the minimum values of the designed experiment (DoE).

4 SUMMARY

To address the gaps in current understanding of the cataphoretic painting process, this study provides valuable insights into the intricate relationships between degreasing temperature, degreasing solution concentration, and applied cataphoretic voltage. Prior research has often oversimplified these variables, leading to suboptimal process optimization and variability in industrial applications. By employing a Design of Experiments (DoE) approach, this study meticulously quantifies the effects of these parameters on layer thickness, uncovering nuances that are critical for the painting process. This research fills a significant gap in understanding the combined effects of degreasing temperature and solution concentration on layer thickness. The data indicates that while higher cataphoretic voltages consistently lead to thicker layers, the optimal thickness is influenced heavily by the concentration of the degreasing solution, with 15 g.L^{-1} proving to be the most effective. This finding highlights a previously underexplored interaction between voltage and concentration, which has implications for process control and quality assurance. The study also reveals how temperature affects layer thickness differently across various concentrations, a detail often overlooked in simpler models. For instance, the notable reduction in thickness at a concentration of 15 g.L^{-1} due to temperature variations underscores the need for precise temperature control in the

degreasing phase. This nuanced understanding helps address gaps in knowledge about temperature's role in layer formation, which is crucial for optimizing process conditions.

The research underscores the critical role of carefully balancing degreasing temperature and solution concentration to achieve desired coating thicknesses. By identifying the concentration of 55 g.L⁻¹ as resulting in the most substantial increase in layer thickness, the study provides actionable insights for adjusting process parameters to enhance coating performance. This level of detail facilitates the development of more precise control strategies, leading to improved consistency and quality in the final product. Furthermore, the findings emphasize the necessity of integrating these parameters into a comprehensive process optimization framework. By acknowledging the complex interplay between voltage, temperature, and concentration, industries can better predict and control the outcomes of the cathoretic painting process.

The results of this study lay a robust foundation for future research aimed at refining the cathoretic painting process. The identified trends and interactions provide a starting point for more detailed investigations into additional variables and their effects on coating quality. In conclusion, this research addresses critical gaps in understanding the cathoretic painting process by elucidating the complex interactions between degreasing temperature, solution concentration, and applied voltage. By doing so, it offers a pathway to optimizing process parameters, ultimately leading to enhanced product quality.

5 ACKNOWLEDGMENTS

This research has been elaborated in the framework of the projects VEGA no. 1/0453/24 and KEGA no. 012TUKE-4/2024 were granted by the Ministry of Education, Science, Research and Sport of the Slovak Republic, project no. APVV-20-0514 granted by the Slovak Research and Development Agency and this publication is the result of the Project implementation: Development of excellent research capacities in the field of additive technologies for the Industry of the 21st century, ITMS: 313011BWN5, supported by the Operational Program Integrated Infrastructure funded by the ERDF.

6 REFERENCES

Akafuah, N.K. et al. Evolution of the Automotive Body Coating Process – A Review. *Journal Coatings*, June 2016, Vol.6, No.2., 24.

Brock, T. et al. *European Coatings Handbook 2nd Edition*. Hannover, Germany: Vincentz Network, 2010. ISBN 978-3-86630-889-3.

Brüggemann, M. and Rach, A. *Electrocoat: Formulation and Technology*. Hannover, Germany: Vincentz Network, 2020. ISBN 978-3-7486-0105-0.

Chung, P.P. et al. Deposition processes and properties on steel fasteners – A review. *Journal Friction*, July 2019, Vol.7, pp 389-416. ISSN 2223-7690.

Ovsik, M. et al. Nano-mechanical properties of surface layers of polyethylene modified by irradiation. *Materials*, 2020, Vol.13, No. 12, 929.

Goeke, S. et al. Enhancing the Surface Integrity of Tribologically Stressed Contacting Surfaces by an Adjusted

Surface Topography. In: 2nd CIRP Conference on Surface Integrity (CSI). *Procedia CIRP*, 2014. pp 214–218.

Goldschmidt, A. and Streitberger, H.J. *BASF Hadbuch Lackiertechnik*. Hannover, Germany Satz: Vincentz Network, 2014. ISBN 978-3-86630-836-1.

Grzesik, W. Influence of Surface Textures Produced by Finishing Operations on their Functional Properties. *Journal of Machine Engineering*, February 2016. Vol.16, No.1., pp 15-23.

Hashimoto, F. et al. Characteristics and Performance of Surfaces Created by Various Finishing Methods. 3rd CIRP Conference on Surface Integrity (CIRP CSI). *Procedia CIRP*, 2016. Vol.45, pp 1-6.

Hawkins, T.R. et al. Comparative Environmental Life Cycle Assessment of Conventional and Electric Vehicles. *Journal of Industrial Ecology*, February 2013. Vol.17, No. 1., pp 53-64.

Holoubek, J. *Cataphoresis painting*. Professional magazine for industry, construction and craftsmen. Praha: Press agency, 2005, (4). ISSN 0551-7354.

Jaczewski, M. et al. *Industrial paint coatings for metal surfaces*. Tikkurila Protective Coating Guide, 2008. TIKKURILA. 2nd edition.

Javidi, A. et al. The Effect of machining on the surface integrity and fatigue life. *International Journal of Fatigue*, October-November 2008, Vol.30, No.10.-11., pp 2050-2055.

Kuracal, P.N. et al. Environmental burdens of cathoretic process. *Journal Desalination and Water Treatment*, December 2019, Vol.172, pp 301-308.

Maaß, P. and Peißker, P. *Handbook of Hot-dip Galvanization*. Wiley-VCH Verlag GmbH and Co. KGaA: Weinheim, Germany, 2011. ISBN 978-3-527-63689-1.

Papasavva, S. et al. Life cycle environmental assessment of paint processes. *Journal of Coatings Technology*, February 2002, Vol.74, No. 925., pp 65-76.

Rivera, J.L. and Reyes-Carrillo, T. A Framework for Environmental and Energy Analysis of the Automobile Painting Process. 21st CIRP Conference on Life Cycle Engineering, *Procedia CIRP*, 2014. Vol. 15, pp 171-175.

Rossi, S. et al. Corrosion protection of aluminium foams by cathoretic deposition of organic coatings. *Journal Progress in Organic Coatings*, 2017, Vol.109, pp 144-151. ISSN 0300-9440.

Skotnicki, W. and Jedrzejczyk, D. The Comparative Analysis of the Coatings Deposited on the Automotive Parts by the Cathoretic Method. *Journal Materials*, October 2021, Vol.14, No.20., 6155.

Skotnicki, W. et al. The influence of the preparation of the surface layer of iron alloys on the mechanical properties of anti-corrosion coatings. *Journal Protection against corrosion*, 2018, Vol.1. pp 29-32. ISSN 0473-7733.

Sternadelova, K. et al. Quality assessment of the vitreous enamel coating applied to the weld joint. *MM Science Journal*, March 2023, Vol. 2023, pp 6333-6338. ISSN 1803-1269.

Votava, J. Anticorrosion protection of strength bolts. *Acta univ.agric. et. Silv. Mendel. Brun.*, 2012, Vol.60, No.1, pp 181-188.